

Rapid adiabatic passage without level crossing

A. A. Rangelov,¹ N. V. Vitanov,² and B. W. Shore³

¹*Department of Physics, Sofia University, James Bourchier 5 blvd., 1164 Sofia, Bulgaria*

²*Department of Physics, Sofia University, James Bourchier 5 blvd.,
1164 Sofia, Bulgaria and Institute of Solid State Physics,*

Bulgarian Academy of Sciences, Tsarigradsko chaussée 72, 1784 Sofia, Bulgaria

³*618 Escondido Cir., Livermore, CA 94550, USA*

(Dated: October 25, 2018)

We present a method for achieving complete population transfer in a two-state quantum system via adiabatic time evolution in which, contrary to conventional rapid adiabatic passage produced by chirped pulses, there occurs no crossing of diabatic energy curves: there is no sign change of the detuning. Instead, we use structured pulses, in which, in addition to satisfying conditions for adiabatic evolution, there occurs a sign change of the Rabi frequency when the detuning is zero. We present simulations that offer simple geometrical interpretation of the two-dimensional motion of the Bloch vector for this system, illustrating how both complete population inversion and complete population return occur for different choices of structured pulses.

PACS numbers: 32.80.Xx, 33.80.Be, 32.80.Qk, 03.65.Ge

I. INTRODUCTION

The technique of rapid adiabatic passage (RAP) [1, 2, 3, 4, 5] provides a well-studied robust and efficient method for producing complete population transfer between two bound states of a quantum system. Traditionally the population change has been accomplished by sweeping the carrier frequency of a laser pulse through resonance with a two-state system (parameterized by detuning), while simultaneously pulsing the strength of the interaction (parameterized as time-varying Rabi frequency). The sweep of detuning corresponds to a crossing of diabatic energy curves, as noted below. When the interaction changes sufficiently slowly, so that the time evolution is adiabatic, there will occur a complete population transfer from the ground state (of energy E_1) to the excited state (energy E_2). Alternatively, one can make the detuning cross resonance by sweeping the transition frequency, e.g. by time-dependent electric or magnetic fields, as exemplified by the recently introduced technique of Stark-chirped rapid adiabatic passage (SCRAP) [6].

In this paper we exploit a novel way of achieving complete population transfer via adiabatic evolution in two-state systems, using pulses that produce no crossing of diabatic energies. Such population transfer is possible when diabatic energy curves touch, but do not cross, and simultaneously there occurs a sign change of the interaction (the Rabi frequency).

II. BACKGROUND

Coherent excitation of a two-state quantum system is described by the time-dependent Schrödinger equation (TDSE), which in the rotating-wave approximation

(RWA) [1, 2] reads

$$i\hbar \frac{d}{dt} \mathbf{C}(t) = \mathbf{H}(t) \mathbf{C}(t), \quad (1)$$

where $\mathbf{C}(t) = [C_1(t), C_2(t)]^T$ is a two-dimensional column-vector whose elements are the probability amplitudes $C_1(t)$ and $C_2(t)$ associated with the two quantum states ψ_1 and ψ_2 , and $\mathbf{H}(t)$ is the matrix representing the RWA Hamiltonian [1, 2],

$$\mathbf{H}(t) = \frac{\hbar}{2} \begin{bmatrix} -\Delta(t) & \Omega(t) \\ \Omega(t) & \Delta(t) \end{bmatrix}. \quad (2)$$

The detuning $\Delta(t) = \omega_0(t) - \omega_L(t)$ expresses the frequency offset of the laser carrier frequency $\omega_L(t)$ from the Bohr transition frequency $\omega_0(t)$, each of which may vary with time. The Rabi frequency $\Omega(t)$ quantifies the field-induced coupling between the two states. For the laser-atom excitation considered here this is the product of the atomic dipole transition moment d_{12} in the field polarization direction, and the electric-field envelope $\mathcal{E}(t)$ of the laser field, $\Omega(t) = -d_{12}\mathcal{E}(t)/\hbar$. We shall take this to be a real-valued function of time.

In writing the RWA Hamiltonian we have chosen a symmetrized form, which is obtained by a suitable phase transformation of the probability amplitudes. The diagonal elements of $\mathbf{H}(t)$ are *diabatic energies*. Curves of diabatic energies cross when $\Delta(t)$ changes sign. The (time-dependent) eigenvalues of $\mathbf{H}(t)$ are *adiabatic energies*, $\hbar\varepsilon_{\pm}(t)$. By definition, $\varepsilon_+(t)$ is the larger of the two eigenvalues.

As has long been known [7], Eq (1) for the two complex-valued probability amplitudes can be recast as three coupled equations for real-valued variables, that serve as the three components of a unit vector $\mathbf{B}(t) = [u(t), v(t), w(t)]^T$ in a three-dimensional abstract space.

The components of this *Bloch vector* are

$$u(t) = 2 \operatorname{Re} \rho_{12}(t), \quad (3a)$$

$$v(t) = 2 \operatorname{Im} \rho_{12}(t), \quad (3b)$$

$$w(t) = \rho_{22}(t) - \rho_{11}(t), \quad (3c)$$

with $\rho_{mn}(t) = C_m^*(t)C_n(t)$ ($n, m = 1, 2$) being the matrix elements of the density operator. The resulting RWA optical Bloch equation reads [1, 2, 7]

$$\frac{d}{dt}\mathbf{B}(t) = \mathbf{R}(t)\mathbf{B}(t), \quad (4)$$

with

$$\mathbf{R}(t) = \begin{bmatrix} 0 & -\Delta(t) & 0 \\ \Delta(t) & 0 & -\Omega(t) \\ 0 & \Omega(t) & 0 \end{bmatrix}. \quad (5)$$

The skew-symmetric nature of the matrix $\mathbf{R}(t)$ allows us to write Eq (4) as a torque equation for the Bloch vector [7, 8],

$$\frac{d}{dt}\mathbf{B}(t) = \mathbf{Q}(t) \times \mathbf{B}(t), \quad (6)$$

where the driving torque (angular velocity) vector $\mathbf{Q}(t)$ reads [7, 8]

$$\mathbf{Q}(t) = [\Omega(t), 0, \Delta(t)]^T. \quad (7)$$

The Bloch vector rotates at the instantaneous rate

$$\tilde{\Omega}(t) = \sqrt{\Omega(t)^2 + \Delta(t)^2}. \quad (8)$$

Note that the direction of rotation will be reversed if the signs of $\Omega(t)$ and $\Delta(t)$ are both reversed.

One of the three eigenvectors of $\mathbf{R}(t)$, which corresponds to a null eigenvalue, is a sum of only two components, the coherence $u(t)$ and the inversion $w(t)$,

$$a_0(t) = u(t) \sin \vartheta(t) + w(t) \cos \vartheta(t). \quad (9)$$

It has no component of $v(t)$; in analogy with stimulated Raman adiabatic passage (STIRAP) [9, 10, 11], we shall refer to it as a *dark vector*. Here the time-dependent mixing angle $\vartheta(t)$ is defined by

$$\tan \vartheta(t) = \Omega(t)/\Delta(t). \quad (10)$$

In contrast to the dark state of STIRAP, the dark vector $a_0(t)$ can radiate via spontaneous emission from the excited state ψ_2 . It is important to note that the components of the dark vector are the normalized components of the torque vector (7).

Below we describe several situations in which the time evolution is adiabatic, so that the Bloch vector *adiabatically follows* the torque vector as, in accord with the design of the functions $\Delta(t)$ and $\Omega(t)$, it moves in a two-dimensional plane of the abstract vector space. The pulses can be designed to produce either complete population inversion (CPI), in which all population resides in state 2 at the completion of the pulses, or complete population return (CPR), in which the initially populated state is completely repopulated after the pulses.

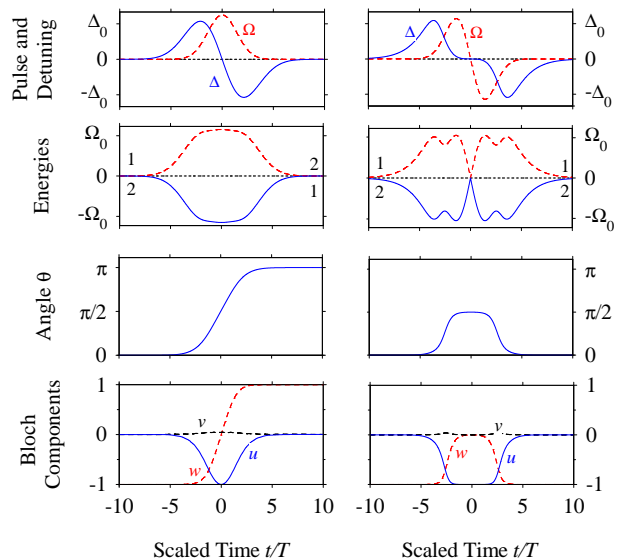


FIG. 1: CPI (left frames) and CPR (right frames) in the presence of level crossing (detuning crossing the resonance). *Left frames:* The detuning and the Rabi frequency are given by Eqs (11), with $\Delta_0 = -40/T$ and $\Omega_0 = 30/T$. *Right frames:* the detuning and the Rabi frequency are given by Eqs (12), with $\tau = 3T$, $\Delta_0 = -25/T$ and $\Omega_0 = -80/T$. *Top frames:* the Rabi frequency and the detuning; *second frames:* eigenenergies; *third frames:* mixing angle $\vartheta(t)$; *bottom frames:* components of the Bloch vector $\mathbf{B}(t)$.

III. ADIABATIC FOLLOWING WITH LEVEL CROSSING

Figure 1 shows examples of adiabatic CPI or CPR in the presence of a level crossing (the detuning crosses the resonance). The frames in the left column of Fig. 1 illustrate CPI for the conventional rapid adiabatic passage (RAP) by a frequency chirped laser pulse [1, 2, 3, 4, 5]. Top frames show the pulsed Rabi frequency and detuning as a function of time, for which we have chosen

$$\Delta(t) = \frac{\Delta_0 t}{T} e^{-(t/1.5T)^2}, \quad (11a)$$

$$\Omega(t) = \Omega_0 e^{-(t/T)^2}, \quad (11b)$$

The second frames show the eigenenergies, the third frames show the mixing angle $\vartheta(t)$, and the bottom frames show the components of the Bloch vector.

The frames in the right column of Fig. 1 illustrate the situation when, in addition to the level crossing of the detuning, the Rabi frequency also changes sign,

$$\Delta(t) = \frac{\Delta_0 t^2}{T^2} \left[\operatorname{sech} \left(\frac{t-\tau}{T} \right) - \operatorname{sech} \left(\frac{t+\tau}{T} \right) \right] \quad (12a)$$

$$\Omega(t) = \frac{\Omega_0 t}{T} e^{-(t/T)^2}, \quad (12b)$$

The temporal pulse area – the time integral of the Rabi frequency – is here zero (a “zero-area pulse”). For this

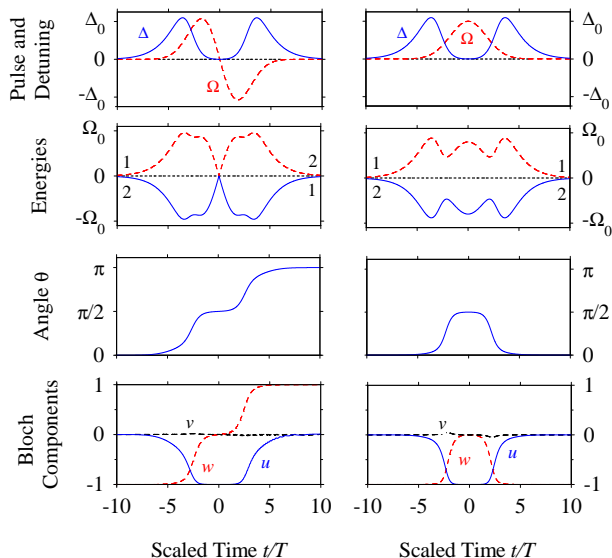


FIG. 2: CPI (left frames) and CPR (right frames) in the absence of level crossing (detuning only touching resonance). *Left frames*: the detuning and the Rabi frequency are given by Eqs (13), with $\tau = 3T$, $\Delta_0 = 4/T$ and $\Omega_0 = -40/T$. *Right frames*: the detuning and the Rabi frequency are given by Eqs (14), with $\tau = 3T$, $\Delta_0 = 4/T$ and $\Omega_0 = 40/T$. *Top frames*: the Rabi frequency and the detuning; *second frames*: eigenenergies; *third frames*: mixing angle $\vartheta(t)$; *bottom frames*: components of the Bloch vector $\mathbf{B}(t)$.

choice of antisymmetric Rabi frequency and detuning, exact CPR takes place. Indeed, this property, which stems from the overall antisymmetry of the Hamiltonian, is valid not only in the adiabatic limit but in the general case, and for arbitrarily many states [12].

For the left frames, during the excitation the mixing angle $\vartheta(t)$ rotates from $\vartheta(-\infty) = 0$ to $\vartheta(0) = \pi/2$ and then to $\vartheta(\infty) = \pi$ (due to the change of the sign of the detuning), which leads to CPI because the system remains in the dark vector (9), which follows adiabatically the driving torque. For the right frames, during the excitation the mixing angle $\vartheta(t)$ rotates from $\vartheta(-\infty) = 0$ to $\vartheta(0) = \pi/2$ and then back to $\vartheta(\infty) = 0$ (due to the change of sign of the detuning and the Rabi frequency at the crossings), which leads to CPR because, again, the system remains in the dark vector (9), but now it has different asymptotics.

The choice of peak amplitudes for the pulses in these examples is such that a measurable value of Bloch vector component $v(t)$ occurs during intermediate stages of the process. As the motion becomes more adiabatic, and the adiabatic following more complete, this component becomes smaller.

IV. ADIABATIC FOLLOWING WITHOUT LEVEL CROSSING

Figure 2 shows a pair of cases, which do not appear to have been reported previously. In the left frames of Fig. 2 we illustrate CPI in the absence of a level crossing, when the detuning does not cross but just touches the resonance. The detuning and the Rabi frequency read

$$\Delta(t) = \frac{\Delta_0 t^2}{T^2} \left[\operatorname{sech} \left(\frac{t+\tau}{T} \right) + \operatorname{sech} \left(\frac{t-\tau}{T} \right) \right], \quad (13a)$$

$$\Omega(t) = \frac{\Omega_0 t}{T} e^{-(t/2.5T)^2}, \quad (13b)$$

During the excitation the mixing angle $\vartheta(t)$ rotates from $\vartheta(-\infty) = 0$ to $\vartheta(\infty) = \pi$, which leads to CPI in the adiabatic limit because the system remains in the dark vector (9). Furthermore for the given example of antisymmetric pulse shape, the time-integrated Rabi frequency (the temporal pulse area) is zero, but the zero pulse area is not a necessary constraint. This is a new approach to CPI, without a level crossing and with a possible zero pulse area.

The right frames of Fig. 2 illustrate the case when the Rabi frequency and the detuning are both even functions of time,

$$\Delta(t) = \frac{\Delta_0 t^2}{T^2} \left[\operatorname{sech} \left(\frac{t+\tau}{T} \right) + \operatorname{sech} \left(\frac{t-\tau}{T} \right) \right], \quad (14a)$$

$$\Omega(t) = \Omega_0 e^{-(t/2.5T)^2}, \quad (14b)$$

The mixing angle $\vartheta(t)$ rotates from $\vartheta(-\infty) = 0$ to $\vartheta(0) = \pi/2$ and then to $\vartheta(\infty) = 0$, which leads to CPI in the adiabatic limit because the system remains in the dark vector (9).

V. DISCUSSION

A. General features

In summary, the analysis above brings us to the following conclusions. CPI takes place in the adiabatic limit when (i) the coupling is an even function of time and the detuning is odd function of time ($\Omega(t) = \Omega(-t)$, $\Delta(t) = -\Delta(-t)$, left frames of Fig. 1), or (ii) the coupling is odd function of time and the detuning is even function of time ($\Omega(t) = -\Omega(-t)$, $\Delta(t) = \Delta(-t)$), left frames of Fig. 2. When (iii) both functions are even function of time or (iv) both are odd function of time, then CPR is observed instead of CPI, right frames of Figure 1 and 2. These findings are summarized in Table I.

We emphasize here that the assumption of definite symmetry of the Rabi frequency $\Omega(t)$ and the detuning $\Delta(t)$, which was made in figures 1 and 2, and summarized in Table I, is only a matter of convenience. In the adiabatic following approximation, which was assumed

Figure	Rabi frequency	detuning	adiabatic limit
	$\Omega(-t)$	$\Delta(-t)$	limit
1 (left)	$\Omega(t)$	$-\Delta(t)$	CPI
1 (right)	$-\Omega(t)$	$-\Delta(t)$	CPR
2 (left)	$-\Omega(t)$	$\Delta(t)$	CPI
2 (right)	$\Omega(t)$	$\Delta(t)$	CPR

TABLE I: Adiabatic limit for fields of particular symmetry: CPI: complete population inversion; CPR: complete population return.

throughout, it is only the *asymptotic* behavior of the *mixing angle* $\vartheta(t)$, which controls the composition of the dark vector (9), that matters.

Because the adiabatic passage is robust, the procedure of CPI with level touching (left frames of Figure 2) is also robust: it depends only weakly on the overlap of the coupling $\Omega(t)$ and the detuning $\Delta(t)$ and their peak values. Moreover, the exact antisymmetry is not required, and high efficiencies can also be achieved with asymmetric time dependences. The only restriction of the pattern that we have to follow in order to achieve CPI is: the detuning starts before the coupling, becomes zero before the coupling changes sign, then rises again with the same sign and ends after the coupling ends.

The torque-equation interpretation of the motion of the Bloch vector provides a useful means of understanding the behaviors discussed above. Figure 3 provides such a picture for the four frames of figures 1 and 2 and Table I. In the adiabatic limit, which we assume, the Bloch vector evolves in the plane (u, w) , which is the $v = 0$ slice of the Bloch sphere. The geometrical representation of the adiabatic evolution of the Bloch vector is easily determined because in the adiabatic limit the state vector coincides with the dark vector (9) and is always parallel or anti-parallel to the driving torque.

B. Experimental feasibility

The concept of a zero-area laser pulse, when first encountered, may seem somewhat confusing. We have discussed such pulses in some detail elsewhere [13]. Here we describe briefly a few of the available techniques.

1. Nonoscillating magnetic fields.

Historically, the concept arose first in nuclear magnetic resonance (NMR), wherein typically spin- $\frac{1}{2}$ particles are controlled by slowly varying magnetic fields [14]. A zero area field can be produced in an obvious manner, by appropriate tailoring of an applied voltage that can reverse the direction of the field and create the desired asymmetric pulse. In NMR the detuning $\Delta(t)$ is replaced by a longitudinal (along the quantization axis) magnetic pulse,

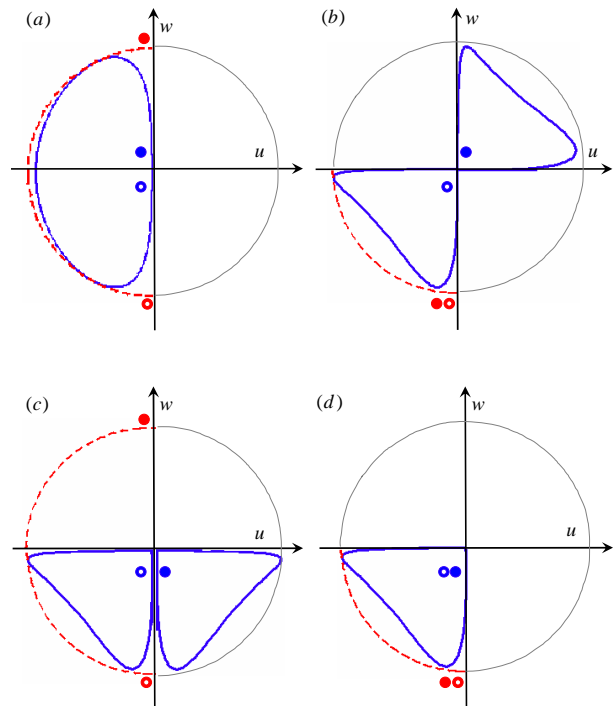


FIG. 3: Motion of the Bloch vector and the angular velocity vector in the (u, w) plane. Solid line (blue online) is the angular velocity (torque) vector, normalized to peak value. Dashed line (red online) is the Bloch vector. The initial positions of the Bloch vector and the torque are marked by hollow circles. The final positions are marked by filled circles. The cases (a)-(d) correspond to the cases of figures 1 and 2.

and the Rabi frequency $\Omega(t)$ by a transverse magnetic pulse.

2. Self-induced transparency.

In the optical spectrum zero-area pulses are formed when pulses are reshaped by self-induced transparency (SIT) while propagating through an absorbing medium. Initial pulse areas in the range $(0, 2\pi)$ will tend toward zero-area pulses – an expression of the McCall-Hahn area theorem [15].

3. Beam splitting & recombination.

A zero-area pulse can also be produced by passing a laser pulse through a beam splitter and then recombining the two split pulses, after delaying one of them by a time delay τ and shifting its phase by π . The recombined pulse, with Rabi frequency

$$\Omega(t) = \Omega_0 [f(t - \tau) - f(t)], \quad (15)$$

where τ is the delay, is a zero-area pulse. Such an implementation requires an interferometric stability within a wavelength λ .

4. Ultrashort shaped pulses.

The most useful techniques, for ultrashort (femtosecond and picosecond) laser pulses, manipulate the Fourier transform of the pulse,

$$\tilde{\Omega}(\Delta) = \frac{1}{2\pi} \int_{-\infty}^{\infty} dt e^{i\Delta t} \Omega(t), \quad (16)$$

using pulse shapers [16]. The pulse area \mathcal{A} is the value of this transform on resonance ($\Delta = 0$),

$$A \equiv \int_{-\infty}^{\infty} dt \Omega(t) = 2\pi\tilde{\Omega}(0). \quad (17)$$

Thus a zero-area pulse can be produced by negating the resonant frequency component $\tilde{\Omega}(0)$ in its spatially dispersed Fourier spectrum.

The desired time variation of the detuning can be produced, using a pulse shaper, *simultaneously* with the manipulation of the Rabi frequency. Alternatively, the pulse of Fig. 2(c) can be produced by shaping the Rabi frequency and the detuning *separately*. For example, the Rabi frequency can still be shaped by a pulse shaper, whereas the detuning can be shaped by manipulating the Bohr transition frequency (rather than the laser carrier frequency through the spectral phase) by using a pair of suitably delayed far-off-resonant Stark-shifting laser pulses, as in SCRAP [6].

C. Comparison with earlier work

CPI with a zero-area pulse has been reported in previous publications [17]. However, the physical mechanisms in these publications is different from the one reported here because the CPI in the present paper relies on adiabatic time evolution at all times. By contrast, in the previous proposals [17] the sudden change of the phase of the

field was essential, which led to sudden evolution, in the form of a delta-function shaped nonadiabatic coupling in the adiabatic basis. This required the use of pulses with large Rabi frequencies, much larger than here.

It is important to note that the zero-area condition is not required in any of these papers because the CPI mechanisms do not require it. The completely antisymmetric shape of the Rabi frequency, $\Omega(-t) = -\Omega(t)$, and the ensuing zero pulse area, is the most natural realization of a function that changes sign at time $t = 0$, but it is by no means necessary for the physical mechanisms.

VI. CONCLUSIONS

We have shown that complete population transfer, by means of adiabatic passage, is possible without any crossing of diabatic energy curves. It is necessary only that the curves touch, and that there be a sign change in the Rabi frequency at that moment. Such a scenario could be used to replace the conventional two-state rapid adiabatic passage via curve crossing for various implementations.

Acknowledgments

This work has been supported by the European Commission projects EMALI and FASTQUAST, and the Bulgarian NSF grants D002-90/08, IRC-CoSiM and Sofia University grant 020/2009.

References

-
- [1] L. Allen, J.H. Eberly, *Optical Resonance and Two-Level Atoms*, Dover, New York, 1987.
 - [2] B.W. Shore, *The Theory of Coherent Atomic Excitation*, Wiley, New York, 1990.
 - [3] N.V. Vitanov, T. Halfmann, B.W. Shore, K. Bergmann, *Annu. Rev. Phys. Chem.* 52 (2001) 763.
 - [4] B.W. Shore, *Acta Physica Slovaca* 58 (2008) 243.
 - [5] N.V. Vitanov, M. Fleischhauer, B.W. Shore, K. Bergmann, *Adv. At. Mol. Opt. Phys.* 46 (2001) 55.
 - [6] L.P. Yatsenko, B.W. Shore, T. Halfmann, K. Bergmann, A. Vardi, *Phys. Rev. A* 60 (1999) R4237; T. Rickes, L.P. Yatsenko, S. Steuerwald, T. Halfmann, B.W. Shore, N.V. Vitanov, K. Bergmann, *J. Chem. Phys.* 115 (2000) 534; A.A. Rangelov, N.V. Vitanov, L.P. Yatsenko, B.W. Shore, T. Halfmann, K. Bergmann, *Phys. Rev. A* 72 (2005) 053403; M. Oberst, H. Münch, T. Halfmann, *Phys. Rev. Lett.* 99 (2007) 173001.
 - [7] R.P. Feynman, F.L.Jr. Vernon, R.W. Hellwarth, *J. Appl. Phys.* 28 (1957) 49.
 - [8] A.A. Rangelov, N.V. Vitanov, B.W. Shore, *J. Phys. B: At. Mol. Opt. Phys.* 42 (2009) 055504.
 - [9] U. Gaubatz, P. Rudecki, S. Schiemann, K. Bergmann, *J. Chem. Phys.* 92 (1990) 5363.
 - [10] K. Bergmann, H. Theuer, B.W. Shore, *Rev. Mod. Phys.* 70 (1998) 1003.
 - [11] N.V. Vitanov, B.W. Shore, *Phys. Rev. A* 73 (2006) 053402.
 - [12] N.V. Vitanov, P.L. Knight, *Opt. Commun.* 121 (1995) 31.
 - [13] B.W. Shore, A.A. Rangelov, N.V. Vitanov, submitted

- Opt. Comm. (2009).
- [14] A. Abragam, The Principles of Nuclear Magnetism, Oxford University Press, Oxford, 1961;
C.P. Slichter, Principles of Magnetic Resonance, Springer, Berlin, 1990.
- [15] S.L. McCall, E.L. Hahn, Phys. Rev. 183 (1969) 457.
- [16] J.C. Diels, W. Rudolph, Ultrashort Laser Pulse Phenomena: Fundamentals, Techniques and Applications on a Femtosecond Time Scale, Academic, San Diego, 1996.
- [17] G.S. Vasilev, N.V. Vitanov, Phys. Rev. A 73 (2006) 023416;
N.V. Vitanov, New J. Phys. 9 (2007) 58;
B.T. Torosov, N.V. Vitanov, Phys. Rev. A 76 (2007) 053404;
F.A. Hashmi, M.A. Bouchene, Phys. Rev. A 79 (2009) 025401.